Technical Report No. 217

036040-10-T

THE MIMI FIELD TEST OF JULY 1970

by

Richard M. Heitmeyer

Approved by: Theodore G. Birdsall
Theodore G. Birdsall

for

COOLEY ELECTRONICS LABORATORY

Department of Electrical and Computer Engineering
The University of Michigan
Ann Arbor, Michigan

Contract No. N00014-67-A-0181-0032
Office of Naval Research
Department of the Navy
Arlington, Virginia 22217

June 1972

ABSTRACT

In the summer of 1970, a field test was conducted to determine if a portable signal processing unit built around a small digital computer could be used to run specific underwater propagation experiments in the Straits of Florida. A periodic broadband signal modulating a 420 Hz carrier was transmitted continuously across the Straits of Florida for nine days. At the receiving site, the power and phase angle of the carrier, the power in the signal sidebands, and the noise power in the signal band were measured. In addition, the total power and the power spectrum in a narrow band about the carrier line were determined as a measure of the modulation due to the forward-scattered surface reverberation. Finally, the correlation of the received signal with a stored reference was computed to measure the multipath structure and its stability. This report presents a brief description of the acoustical range, the experiments, and the preliminary analysis of the data.

ACKNOWLEDGMENTS

The field test described in this report was conducted as part of Project MIMI (The University of Michigan, University of Miami) propagation and signal processing research sponsored by Code 468 of the Office of Naval Research. The field test was jointly conducted by the Acoustics Group of the Rosenstiel School of Marine and Atmospheric Sciences (RSMAS), University of Miami, under the direction of Dr. John Steinberg, and by the Signal Processing Group of Cooley Electronics Laboratory (CEL), The University of Michigan, under the direction of Dr. Theodore G. Birdsall.

The Acoustics Group at RSMAS as a whole deserves special credit for not only maintaining the Miami-Bimini range but also for providing invaluable background information of the propagation conditions in the Straits of Florida. Special thanks go to Mr. Theodore Crabtree who did an excellent job of maintaining the equipment at the Bimini receiving site.

The signal processing techniques used in the experiment were developed by Dr. Birdsall. Messrs. Kurt Metzger, Gerald Cederquist, Peter Wood and Brian Barton also made major contributions to the signal processing effort.

TABLE OF CONTENTS

LIST OF ILLUSTRATIONS

LIST OF ILLUSTRATIONS (Cont.)

Chapter 1

THE MIMI FIELD TEST OF JULY 1970

In the summer of 1970, a field test was conducted to determine if a portable signal processing unit built around a small digital computer could be used to run specific underwater propagation experiments in the Straits of Florida. A periodic, broadband signal, modulating a 420 Hz carrier was transmitted continuously across the Straits of Florida for nine days. At the receiving site, the power and phase angle of the carrier, the power in the signal sidebands, and the noise power in the signal band were measured. In addition, the total power and the power spectrum in a narrow band about the carrier frequency were determined as a measure of the modulation due to the forward-scattered surface reverberation. Finally, the correlation of the received signal with a stored reference was computed to measure the multipath structure of the channel and its stability.

During the course of the experiment approximately 2 million digital words of the reception were recorded for later processing. This report, however, contains only the description of the different experiments and the preliminary analysis of the on-line results. A more complete report on the results of additional processing of the data is planned.

1.1 The Miami-Bimini Range

Location and Facilities. The Miami-Bimini range, illustrated in Fig. 1, is part of the facilities of the Acoustics Group of the Rosenstiel School of Marine and Atmospheric Sciences (RSMAS) of the University of Miami.[1] It extends across the Straits of Florida from Miami to Bimini, Bahamas.

The transmitting site is located at Fowey Rocks [point 2, Fig. 1(a)] approximately 12 miles from the RSMAS laboratory. At the transmitting site, which is connected to the RSMAS laboratory by telephone lines (point 1, Fig. 1), a bottom mounted projector is located in 72 feet of water at the focal point of a 24 ft. compliant tube, parabolic reflector. It has a maximum output level of 120 dB/ μbar at one meter with a nominal bandwidth of 100 Hz. The 30^{o} beamwidth is directed toward Bimini, a distance of 43 nautical miles.

Two receiving sites were used in the experiment. At the first of these, a bottom mounted hydrophone is located in 1000 feet of water at point 4 in Fig. 1(a) approximately 7 miles from the source. The reception from this hydrophone is transmitted to the RSMAS laboratory by marine cable. This site is hereafter referred to as the 7-mile hydrophone site. The second receiving site is located off Bimini at point 3 (Fig. 1). There, a bottom mounted hydrophone

---

[1] J. C. Steinberg and T. G. Birdsall, "Underwater Sound Propagation in the Straits of Florida," J. Acoust. Soc. Am., 39, 301-315 (1966).

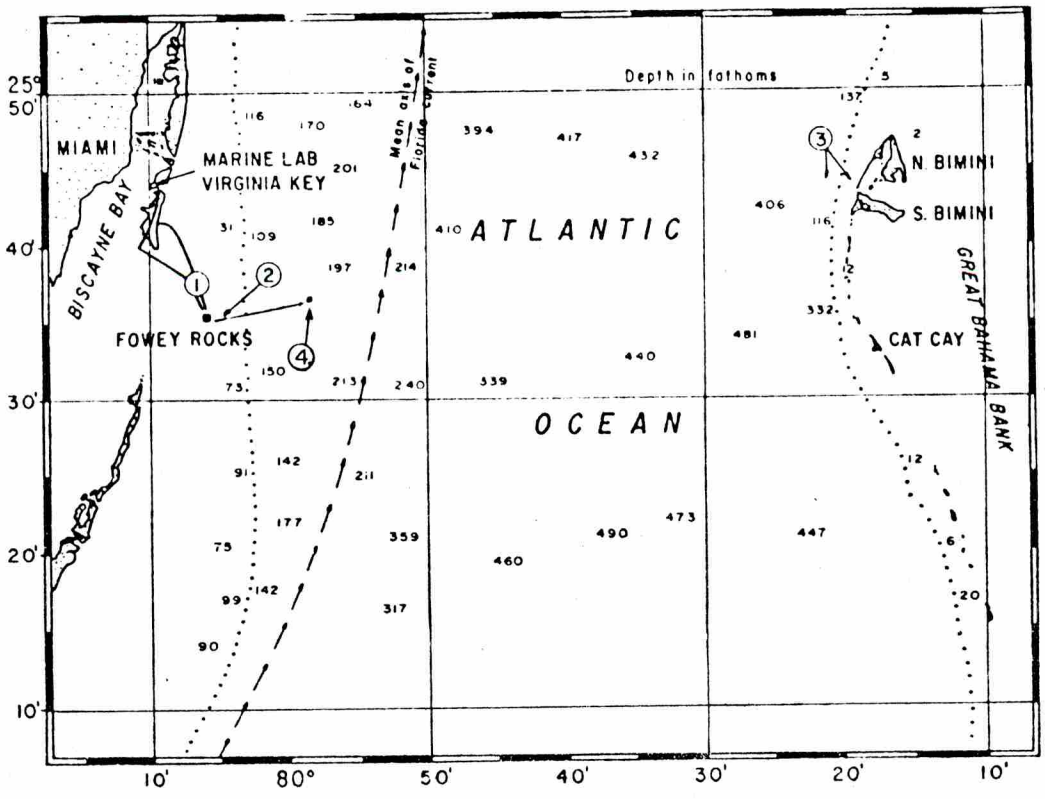

(a)

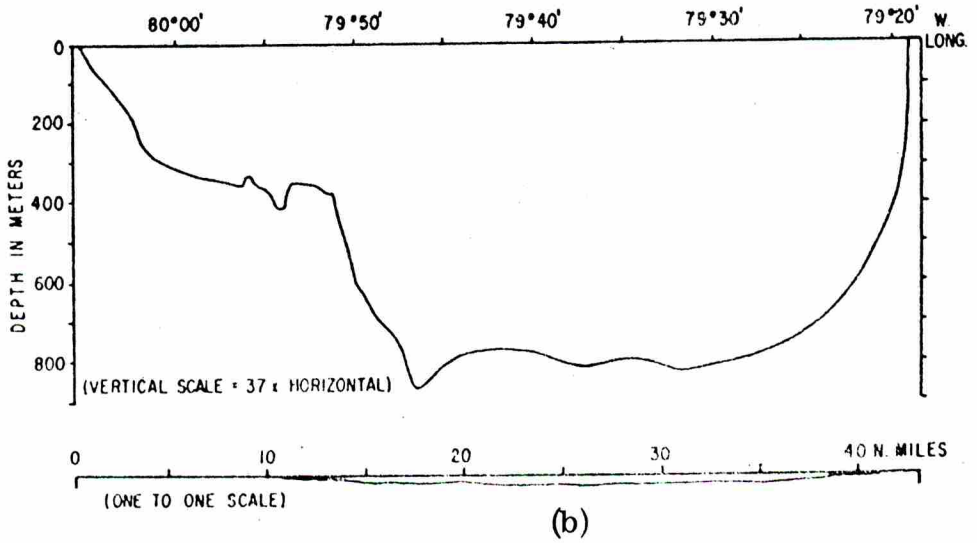

(b)

Fig. 1. The Miami-Bimini range: (a) the Straits of Florida, (b) bottom profile

is located at a depth of 1200 feet and cable-connected to Lerner Marine Laboratory on Bimini, a distance of about 2 miles. This site is referred to as the Bimini hydrophone site. Only one of the two receiving sites was used at a time.

Oceanographic and Acoustical Characteristics. The bottom profile of the Miami-Bimini range is illustrated in Fig. 1(b). A shelf extends out from Miami about 15 miles to a depth of 400 meters followed by a sharp drop-off to a depth of 800 meters. Thirty miles beyond, the Grand Bahamas bank rises abruptly from this depth.

A velocity profile, obtained during April 1961 but which is also typical of the summer conditions, appears in Fig. 2. This profile is characterized by a mixed layer which extends to the relatively constant depth of 100 meters followed by a region of negative velocity gradient. It is noted that the velocity gradient becomes increasingly negative as the Florida shore is approached.

The ray diagram corresponding to the velocity profile of Fig. 2 is shown in Fig. 3. This diagram shows sound being propagated by reflections from surface and bottom and by refraction and reflection from the bottom.

1.2 The Transmitted Signal

The transmitted signal consisted of a linear-maximal, pseudo-random sequence used to complement-phase modulate (CM) a carrier.

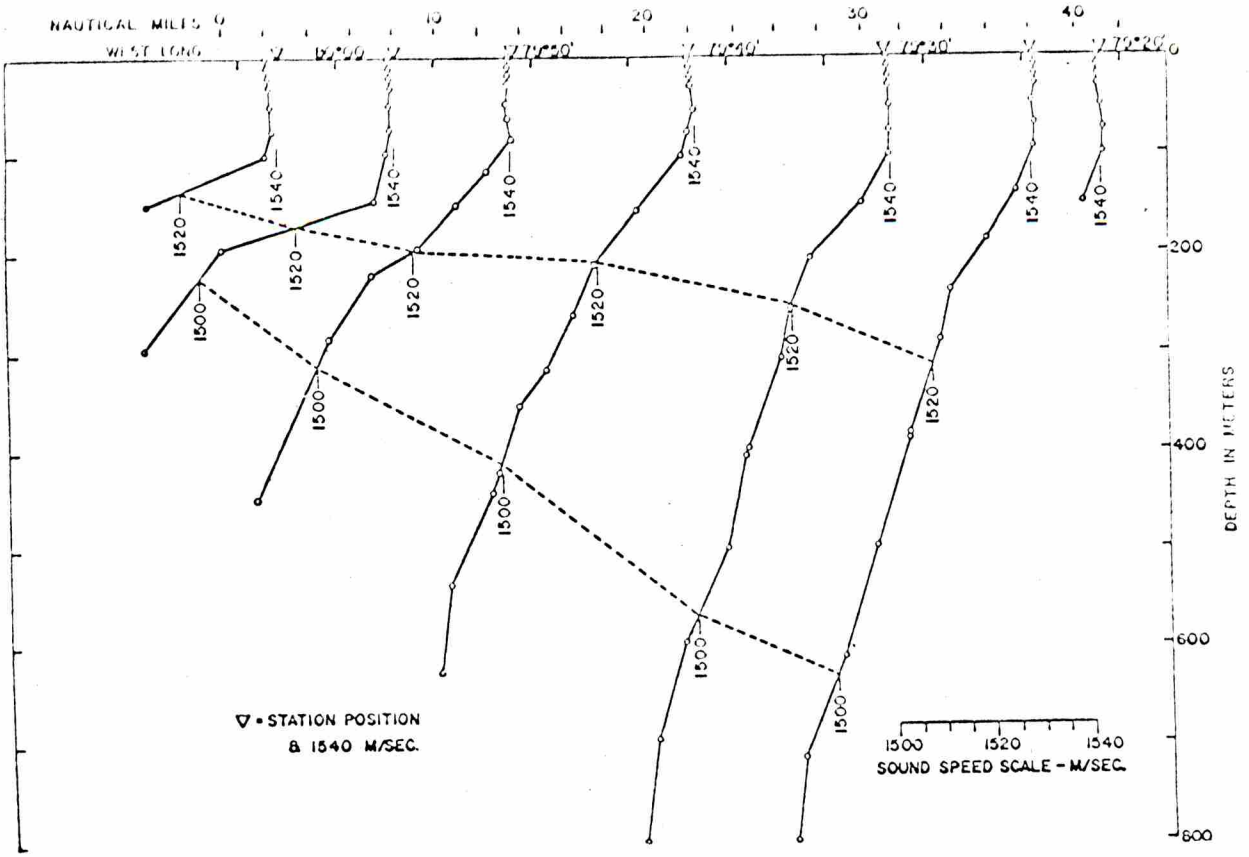

Fig. 2. Sound speed vs depth, Miami to Cat Cay, 26-27 April 1961

The phase of the carrier is shifted to either $+45^{o}$ or -45^{o} depending on the value of the binary digit in the modulating sequence. A portion of a CPM signal is shown in Fig. 4 where:

f_c = carrier

d = duration of the sequence digit

D = number of cycles of carrier per sequence digit

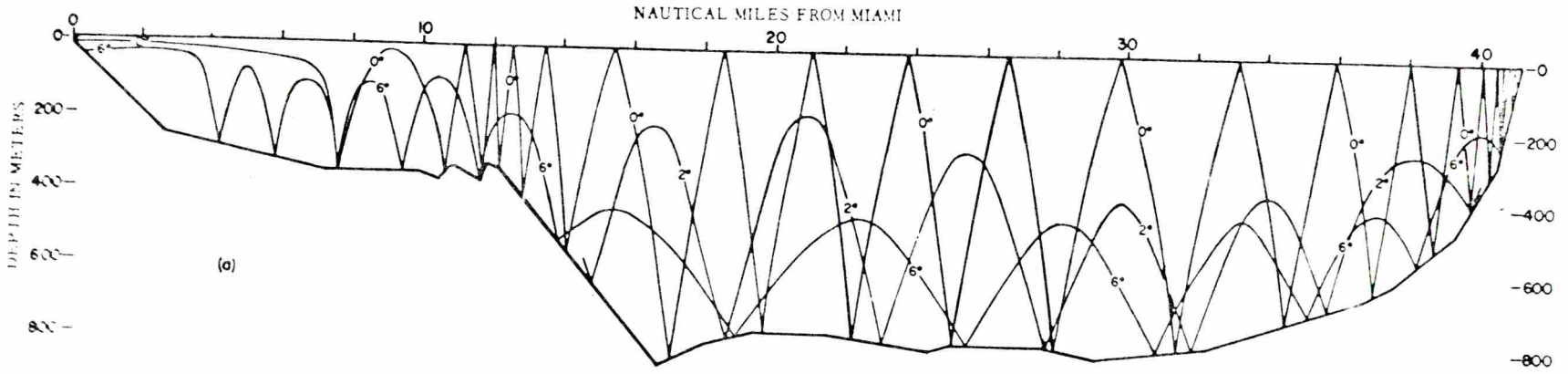

Fig. 3. Sound ray paths along 25° 44' on 26-27 April 1961

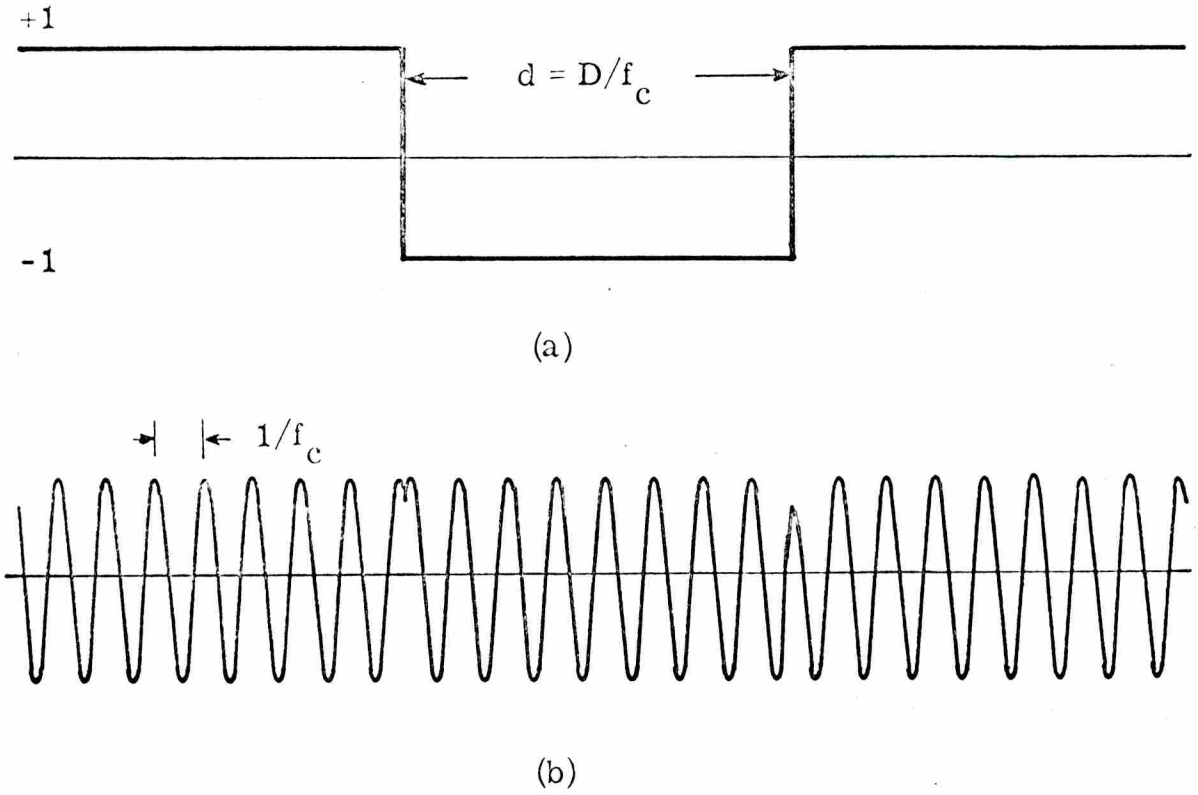

Fig. 4. A complement-phase modulated signal
(a) a portion of the modulating waveform
(b) the resulting transmission

Evidently

$$d = D/f_c$$

Furthermore, when the number of cycles of carrier per digit D is integer-valued, the signal is periodic with period

$$T = Ld = LD/f_c$$

where L is the number of digits in one period of the modulating sequence.

The RMS power spectrum of a typical (CPM) signal is shown in Fig. 5 for the special case $L = 15$ and $D = 8$. It is seen that this spectrum has a $\sin(x)/x$ envelope except at the carrier frequency. It can easily be shown that approximately half of the total power is contained at the carrier frequency with the other half contained in the sideband frequencies.

For the specific signal used in the experiment,

$$f_c = 420 \text{ Hz}$$

$$D = 8 \text{ cycles/digit}$$

and

$$L = 63 \text{ digits}$$

with the result that the digit duration and the period were

$$d = 0.019 \text{ seconds}$$

and

$$T = 0.59 \text{ seconds}$$

Furthermore, the frequency line spacing Δf and the effective signal band B (frequency spread between the spectral zeros on either side of the carrier) were

$$\Delta f = 1/T = 1.69 \text{ Hz}$$

$$B = 2/d = 105 \text{ Hz}$$

Finally, it can be shown that there are 61 spectral lines lying within the signal band.

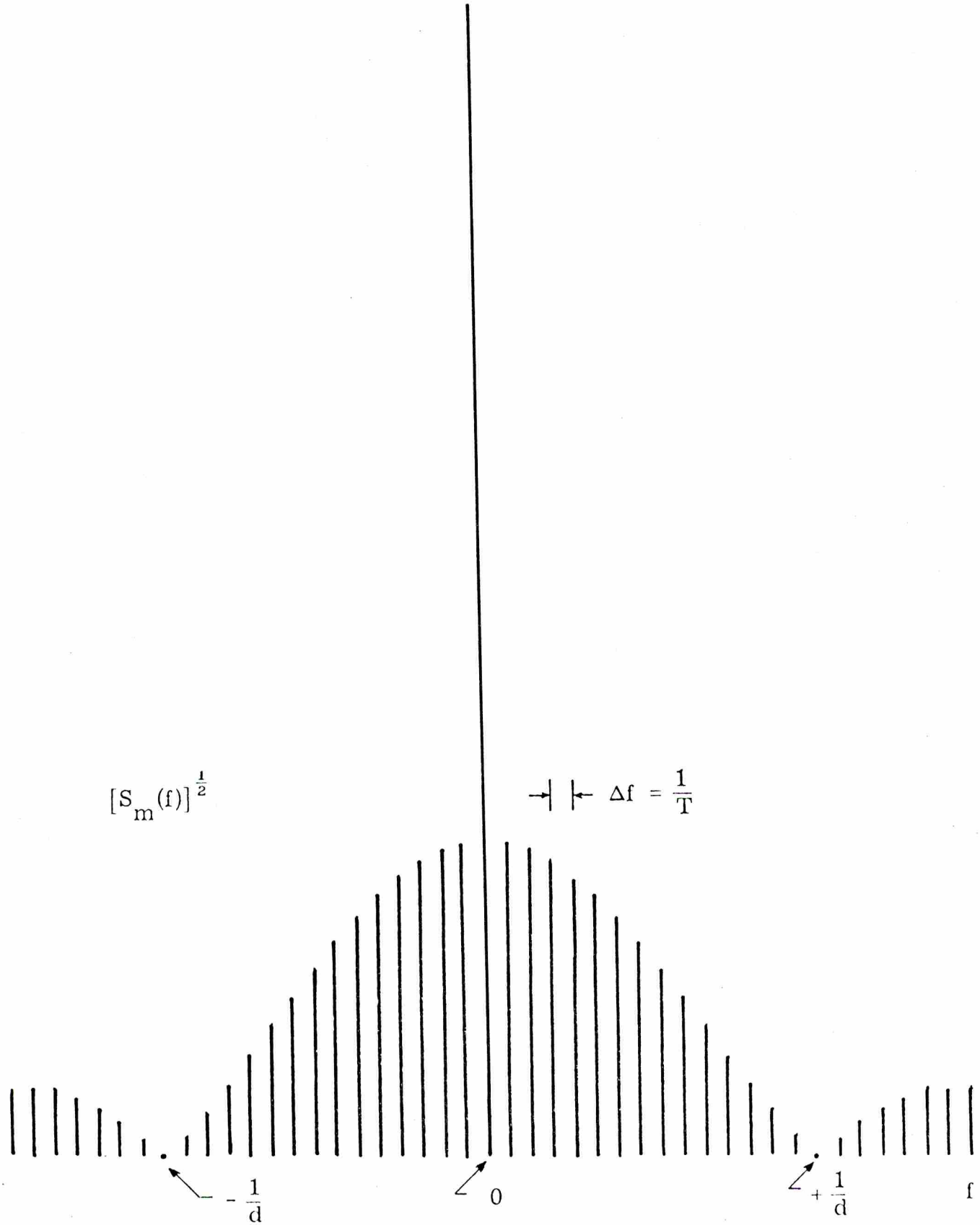

Fig. 5. The RMS spectrum of a complement-phase modulated signal for L = 15 and D = 8

1.3 The Quantities Measured

Three different experiments were conducted during the July 1970 field test: (1) a signal power, noise power and carrier angle experiment, (2) a forward-scattered surface reverberation experiment, and (3) a multipath structure experiment. The measurements in each of the experiments were obtained using digital processing techniques implemented by a digital computer located at each receiving site (Section 1.4). Each of the measurements is computed and recorded every 75 seconds on the basis of the full 75 seconds of data except for the reverb spectrum (Section 1.3.2), which is computed every 125 seconds.

1.3.1 Powers and Angle Experiment.

C Power. The C power measurement is a measure of the power present in the carrier of the received signal. It is determined as that power passing through a digital processing filter with a frequency response, $H_C(f)$, as illustrated in Fig. 6(a).[2] Note that due to the narrow bandwidth,[3] (13.24 MHz), $H_C(f)$ passes only the carrier frequency and none of the sideband frequencies present in the spectrum of the transmitted signal.

---

[2] Only the main lobes of the frequency responses of the processing filters in Fig. 6 are illustrated since these lobes contain almost all of the total power.

[3] By bandwidth we mean one-half the frequency spread between the two zeros on either side of the center frequency of the main lobe.

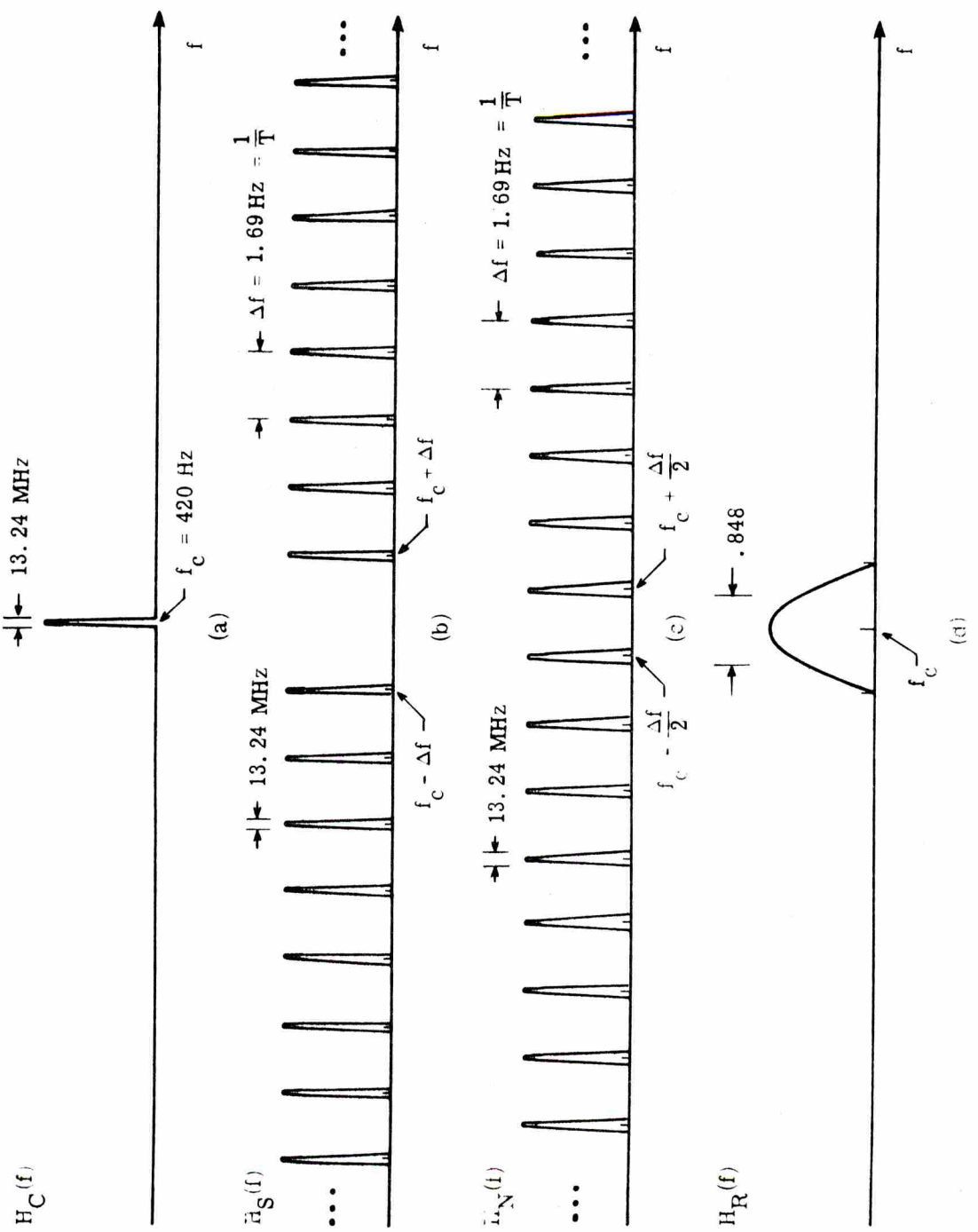

Fig. 6. The frequency responses of the digital processing filters

N Power. The N power measurement is a measure of the noise power contained within the signal band: $f_c - B/2 \leq |f| \leq f_c + B/2$. It is determined as that power passing through the digital processing filter with a frequency response, $H_N(f)$, as illustrated in Fig. 6(c). Such a filter is often referred to as a comb filter. Note that each "tooth" in $H_N(f)$ is centered midway between the spectral lines in the signal spectrum, and the bandwidth of each tooth is again 13.24 MHz.

S Power. The S power measurement is a measure of the signal power within the signal band, excluding the carrier power. It is determined as that power passing through the digital processing filter with frequency response $H_S(f)$ as illustrated in Fig. 6(b). This filter is recognized as a comb filter with a tooth missing at the carrier frequency. The remaining teeth are aligned with the line frequencies of the transmitted signal. The bandwidth of each tooth is 13.24 MHz.

Carrier Angle (A). The carrier angle is a measure of the relative difference between the phase of the output of the carrier processing filter and the phase of the local reference oscillator (Section 1.4).

1.3.2 Surface Reverberation Measurements. The effect of surface reverberation is to scatter some of the power of a transmitted

frequency into sidebands on either side of that frequency. It is felt that this scattered power should lie between 0.1 Hz and 0.4 Hz on either side of the transmitted frequency, depending on the spectrum of the surface waves. For the signal used in the experiment, the spacing between the lines in the power spectrum is $\Delta f = 1.69$ Hz so that the sideband line frequencies do not interfere with the power scattered from the carrier frequency. Thus, the effect of surface reverberation can be measured by computing the power spectrum at the output of the processing filter whose frequency spectrum, $H_R(f)$, is shown in Fig. 6(d). Note that the bandwidth of $H_R(f)$ is large enough to include the power scattered by surface reverberation but small enough to exclude the power in the signal sidebands.

In addition to computing the reverberation or "reverb" spectra, the total power at the output of $H_R(f)$ minus the carrier power is also computed. This power, referred to as the reverb power or R power, is a measure of the power in the sidebands of the reverb spectrum.

1.3.3 Multipath Structure Measurements. The magnitude of the cross-correlation function between the demodulated reception and a pulse-compression reference is computed to measure the multipath structure of the channel. In the absence of noise, this function has a triangular peak of width, $2d = 0.038$ seconds, centered at the arrival time of each transmission path, mod(T), and an amplitude proportional

to the amplitude of the signal received over that path. For example, the cross-correlation function for the special case of only two transmission paths is shown in Fig. 7. Note that this is the same function as would be obtained if a single, large, one-digit pulse were transmitted once every T seconds and received through a matched filter.

As a measure of the time stability of the channel multipath structure, the zero-delay complex cross-correlation coefficient between the demodulated received signal and a previously stored replica of the received signal is calculated for each data set. When this coefficient falls below a set value, indicating a marked change in the multipath structure, the current signal becomes the replica, and the new multipath picture is displayed. Otherwise, the previous replica is displayed and retained in storage. The changing magnitude of the correlation coefficient is an indication of how fast the multipath structure is changing.

1.4 The Equipment Configuration

The configuration of the equipment used in the experiment is shown in Figs. 8 and 9. Figure 8 illustrates the configuration used in the generation and transmission of the signals and in the processing of the reception from the 7-mile phone at Miami. Figure 9 shows the configuration used in the processing of the reception at Bimini.

The operation of the equipment in Fig. 8 is as follows. The frequency standard (accurate to 1 part in 10^{10}) provides a 100 kHz

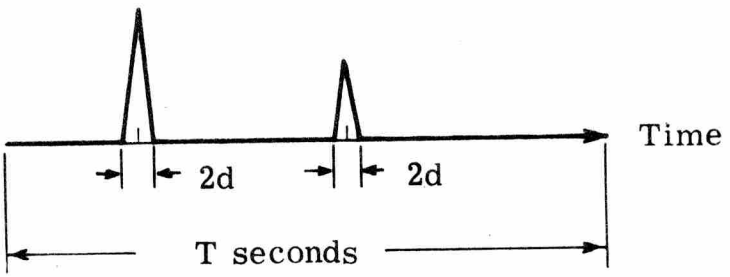

Fig. 7. A multipath display for two transmission paths

reference signal which is converted to a 1680 Hz (= 4x carrier frequency) clock signal by the frequency synthesizer and then passed through an isolation amplifier. One output of the isolation amplifier is used as a reference for the digital modulator whose output, after filtering, is the CPM signal described in the preceding section. This signal is amplified and then transmitted down the Miami-Bimini range. The reception at the 7-mile hydrophone is amplified and transmitted back to the RSMAS laboratory. There it is filtered and amplified and then processed by the FIELD-8 computer. The other output of the isolation amplifier provides a clock signal to the FIELD-8 computer for use in sampling the reception.

The receiving equipment at Bimini (Fig. 9) operates in essentially the same way as the receiving equipment at Miami. The

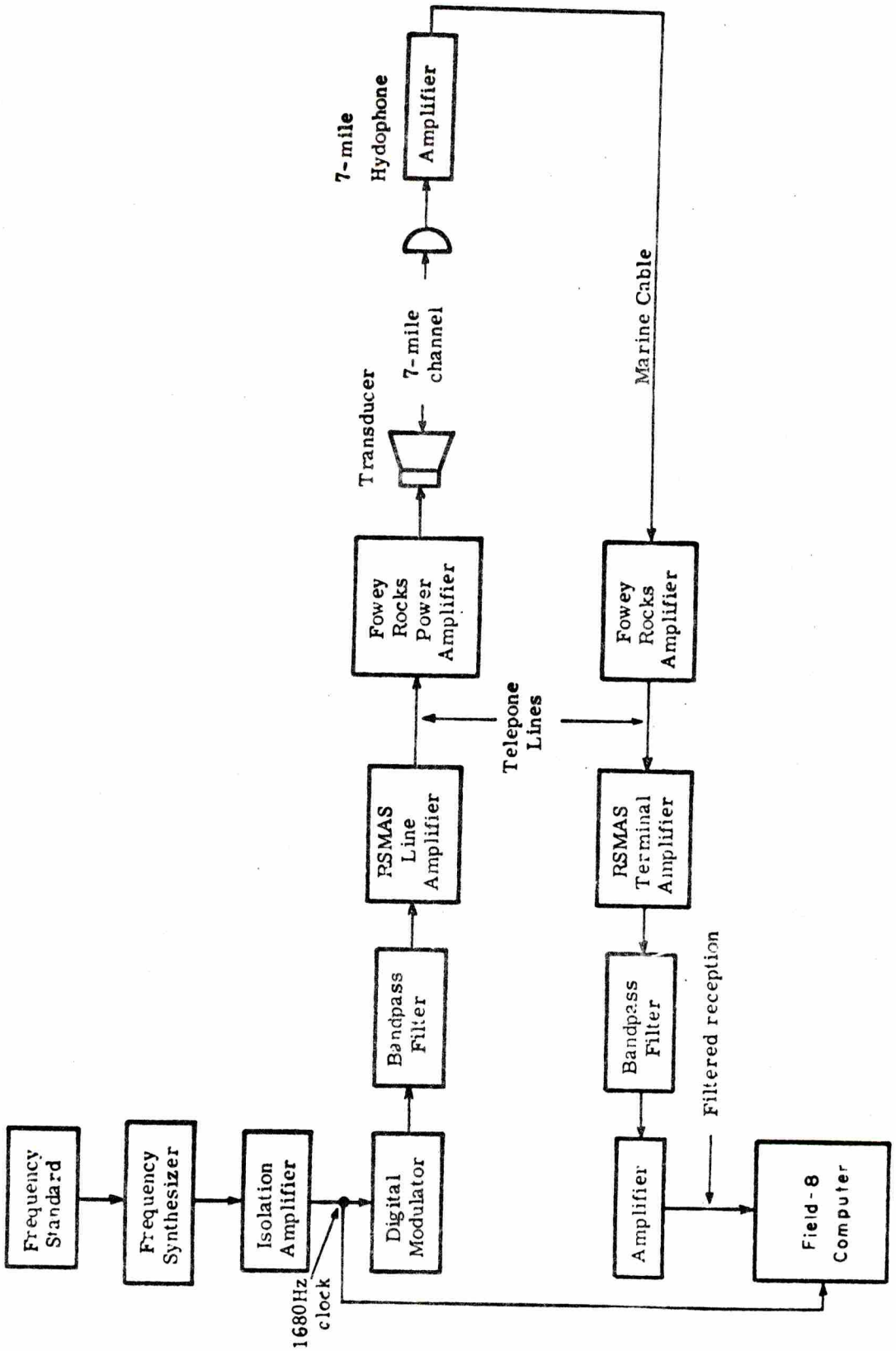

Fig. 8. Equipment configuration at RSMAS (Miami)

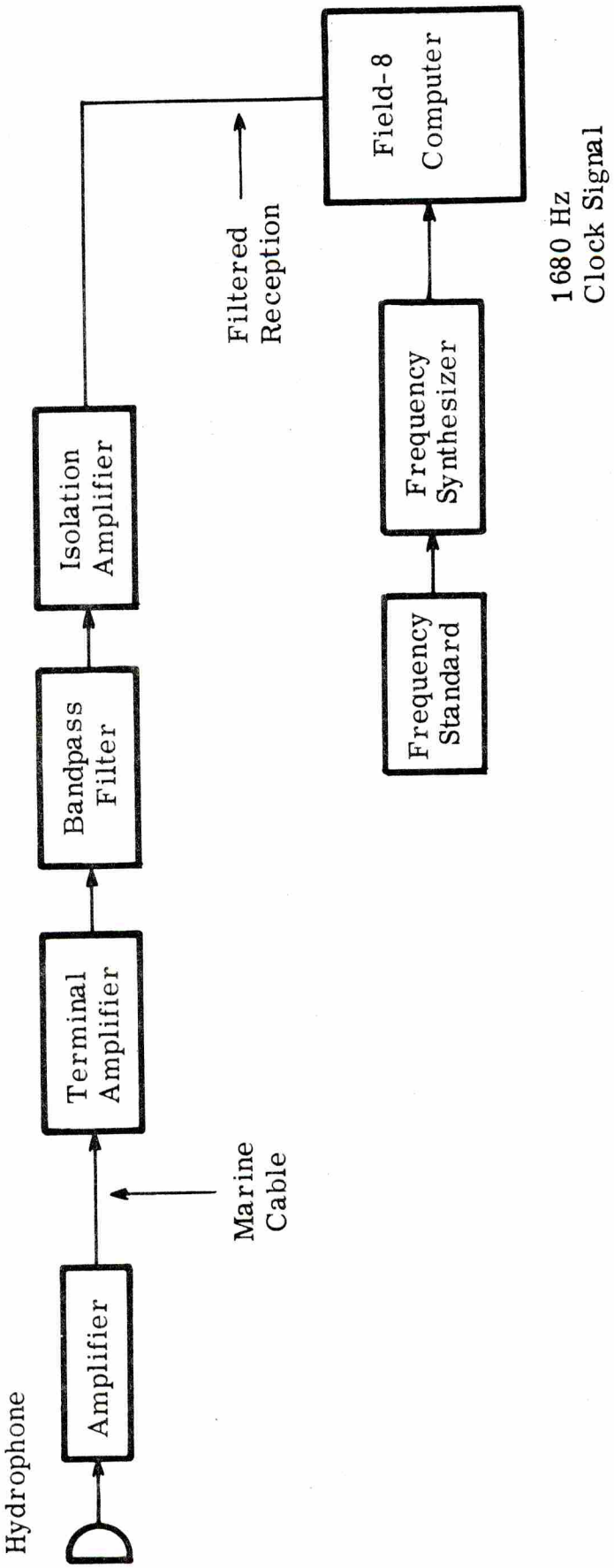

Fig. 9. Equipment configuration at Bimini

reception from the hydrophone is transmitted to the Lerner Marine Laboratory at Bimini, amplified and filtered and then processed by the FIELD-8 computer. The coherent clock signal for the computer is obtained from a frequency standard and synthesizer identical to that employed at Miami.

The FIELD-8 computers shown in Figs. 8 and 9 are used to implement the processing filters and to calculate the reverb spectrum and multipath displays as discussed in Section 1.3. In this capacity, the FIELD-8 functions as indicated in Fig. 10. The FIELD-8 computer itself, consists of a modified PDP-8 with special peripherals to display and store the data. During the July 1970 field test only one of these units was available so that it was necessary to transport it from one receiving site to the other.

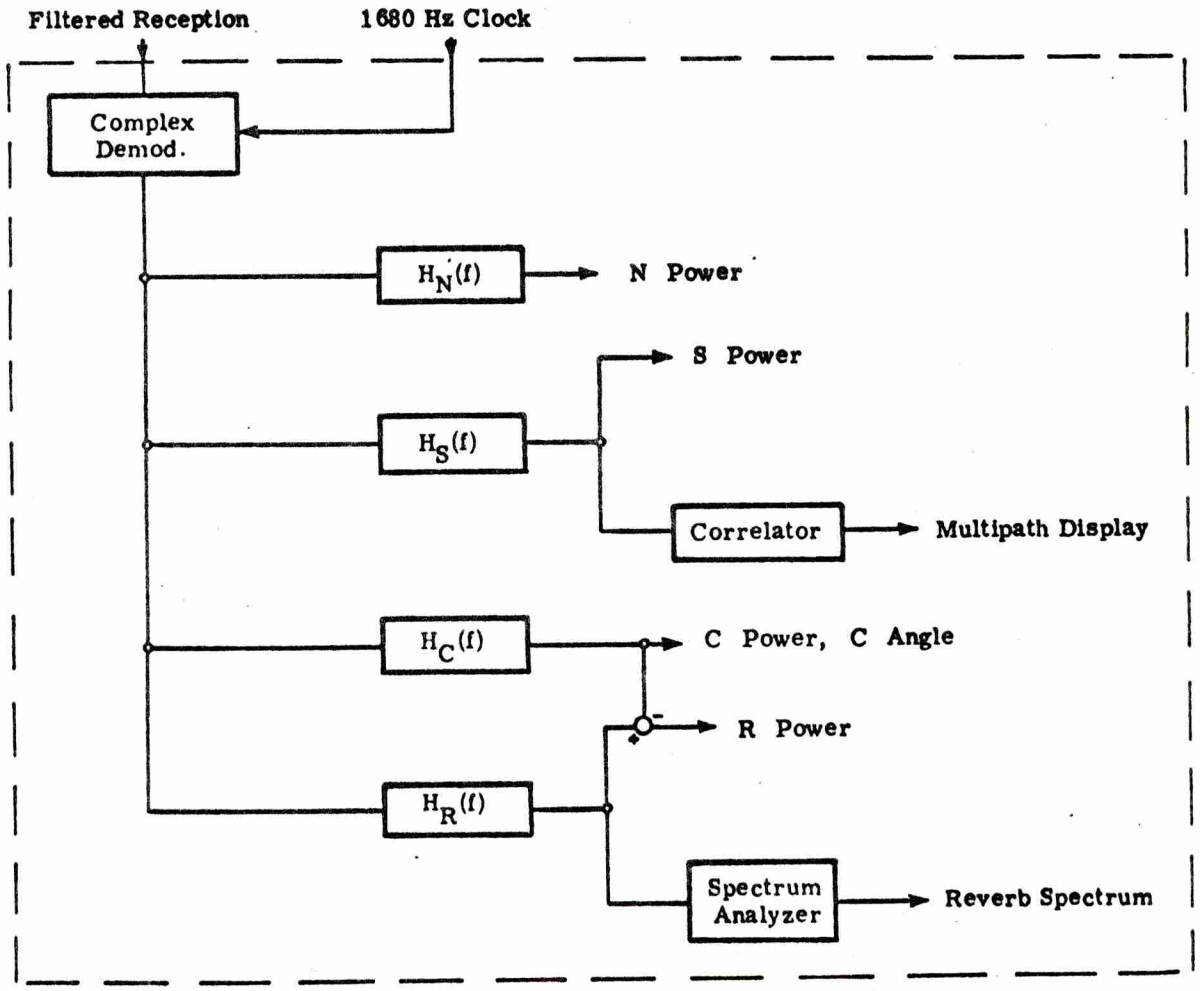

Fig. 10. Block diagram of the digital processing implementation

Chapter 2

THE PRELIMINARY ANALYSIS OF THE JULY 1970 FIELD TRIP

Both the power and angle experiment and the reverb experiment were run over the 7-mile hydrophone for a 24-hour period. At Bimini, all three experiments were conducted over an 8-day period. This chapter presents the preliminary analysis of the data from those experiments.

2.1 The Power and Angle Measurements

Examples of the power measurements, expressed in decibels relative to an arbitrary reference, have been plotted as continuous functions of time. (Continuity has been obtained by linear interpolation between the discrete data points.) Two different vertical scales have been used. In the one case, the vertical scaling is determined as if the gain of each of the processing filters in Fig. 6 is equal to unity. These plots are referred to as the unity-gain plots (UG). In the other case, the vertical scaling has been determined as if the product of the gain and the bandwidth of each of the processing filters is constant. These plots are referred to as the constant gain-bandwidth (CGB) plots. The CGB plots have the property that the approximate signal-to-noise ration (in dB) at the output of the processing filters $H_C(F)$, $H_S(f)$ and $H_R(f)$ can be obtained simply by

subtracting N power from C , S or R power respectively.

Figure 11 illustrates a CGB plot of the power measurements from the Bimini hydrophone taken over a period of 9-1/2 hours. It is seen that the carrier power varies over a wide range with most of the variation appearing as sharp, deep fades occurring at a rate of about two fades per hour. The sideband power is considerably more stable than the carrier power with all of the variation limited to a 10 dB range. Note that there appears to be little correlation between the sideband power and the carrier power. Typical signal-to-noise ratios for the carrier power and the sideband power are 30 dB and 15 dB respectively.

The Bimini noise power in Fig. 11 varies over a range of 25 dB during the 9-1/2 hour period. Part of this variation appears as sharp isolated peaks that can be attributed to the local shipping noise. The remainder appears as slowly varying changes in the average level. The reverb power exhibits the same general behavior as the noise power with a signal-to-noise ratio of approximately 6 dB.

Figure 12 illustrates a CGB plot of the power measurements from the 7-mile hydrophone. It is noted that although there are deep fades in the 7-mile carrier power, they occur at a considerably lower rate than in the Bimini carrier power. In the 9-1/2 hour period illustrated in Fig. 12 there are only 5 deep fades. The 7-mile sideband

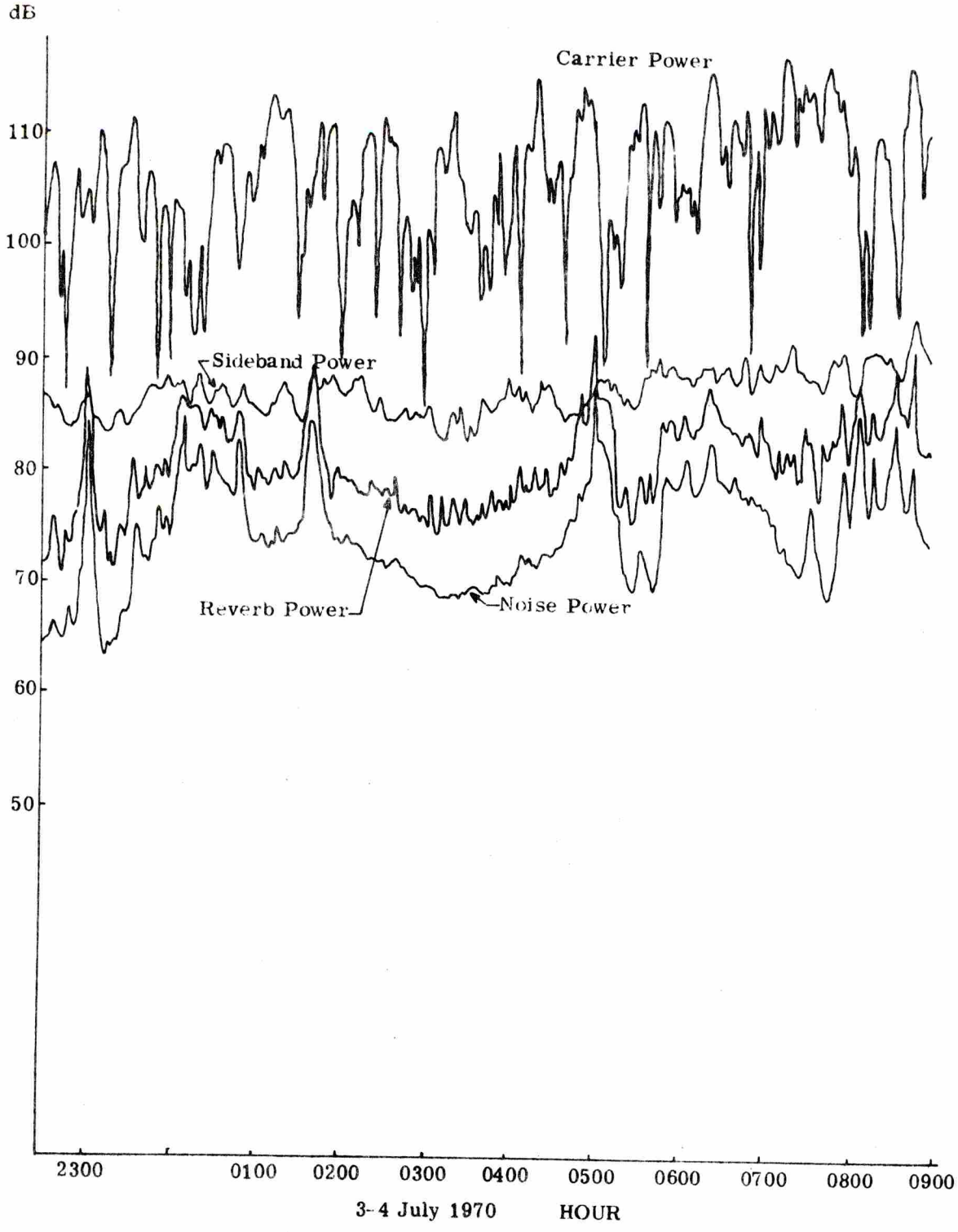

Fig. 11. Power measurements from the Bimini hydrophone

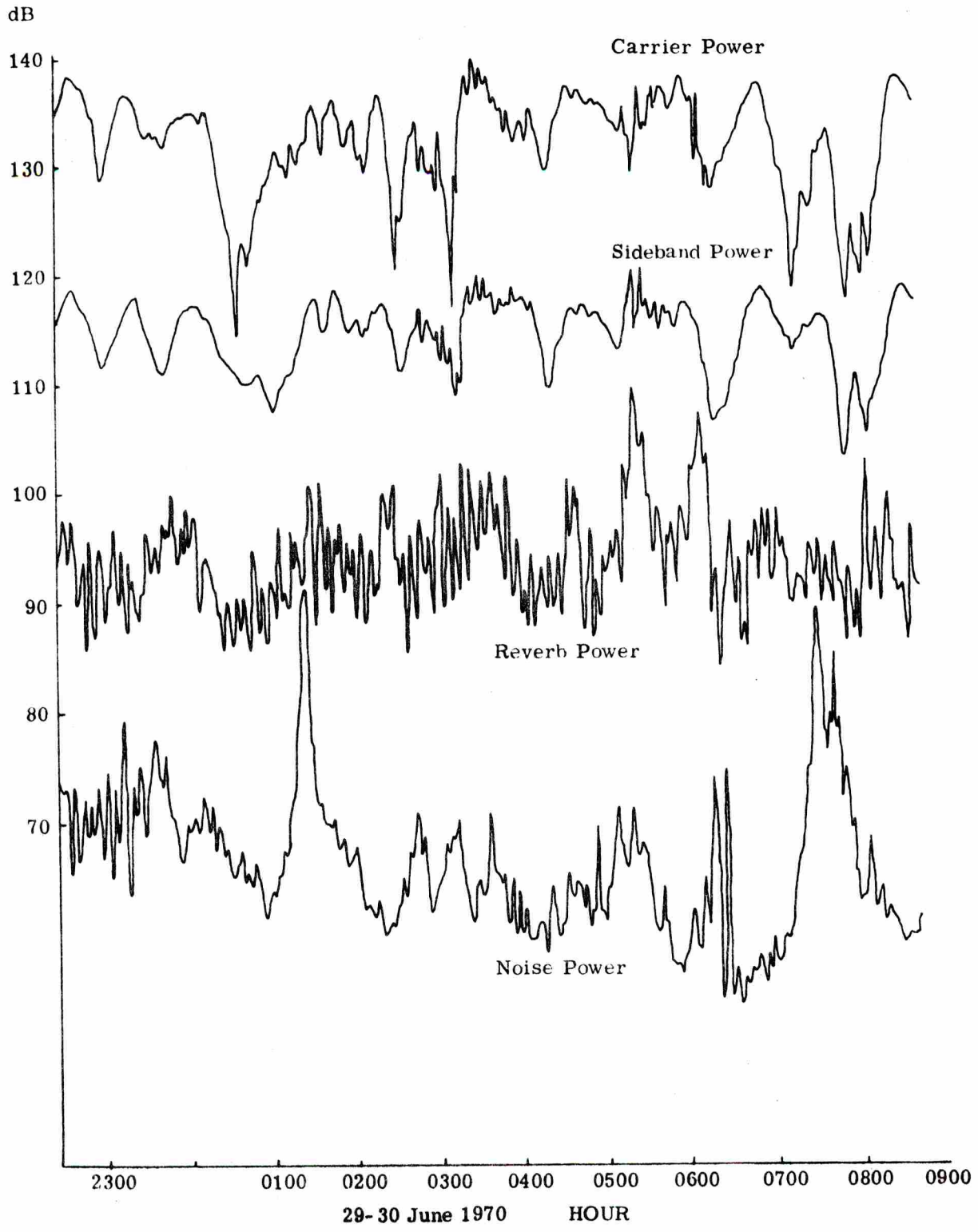

Fig. 12. Power measurements from the 7-mile hydrophone

power, however, appears to be less stable than the Bimini sideband power. There are several periods during which the 7-mile sideband power varies more than 10 dB in less than an hour. Typical signal-to-noise ratios for the 7-mile carrier power and sideband power are 60 dB and 50 dB respectively.

The 7-mile noise power in Fig. 12 has the same general character as the Bimini noise power. Again there are several large shipping noise spikes and some slowly varying changes in the mean noise level. There does, however, seem to be a component of high frequency variation not contained in the Bimini noise power.

The 7-mile reverb power in Fig. 12 differs radically from the Bimini reverb power. The reverb signal-to-noise ratio is over 20 dB and there appears to be little correlation with the noise power. Also there is a significant amount of high frequency variation in the 7-mile reverb power that is not present in the Bimini reverb power.

The most striking distinction between the power measurements at the two receiving sites is the amount of correlation between the carrier power and the sideband power. The two Bimini powers show little if any correlation, whereas, the carrier power and the sideband power from the 7-mile hydrophone show a high degree of correlation. This distinction is most apparent in Fig. 13 which illustrates the two powers from both receiving sites plotted on a UG scale.

The plot of the Bimini powers in Fig. 11 illustrates only a

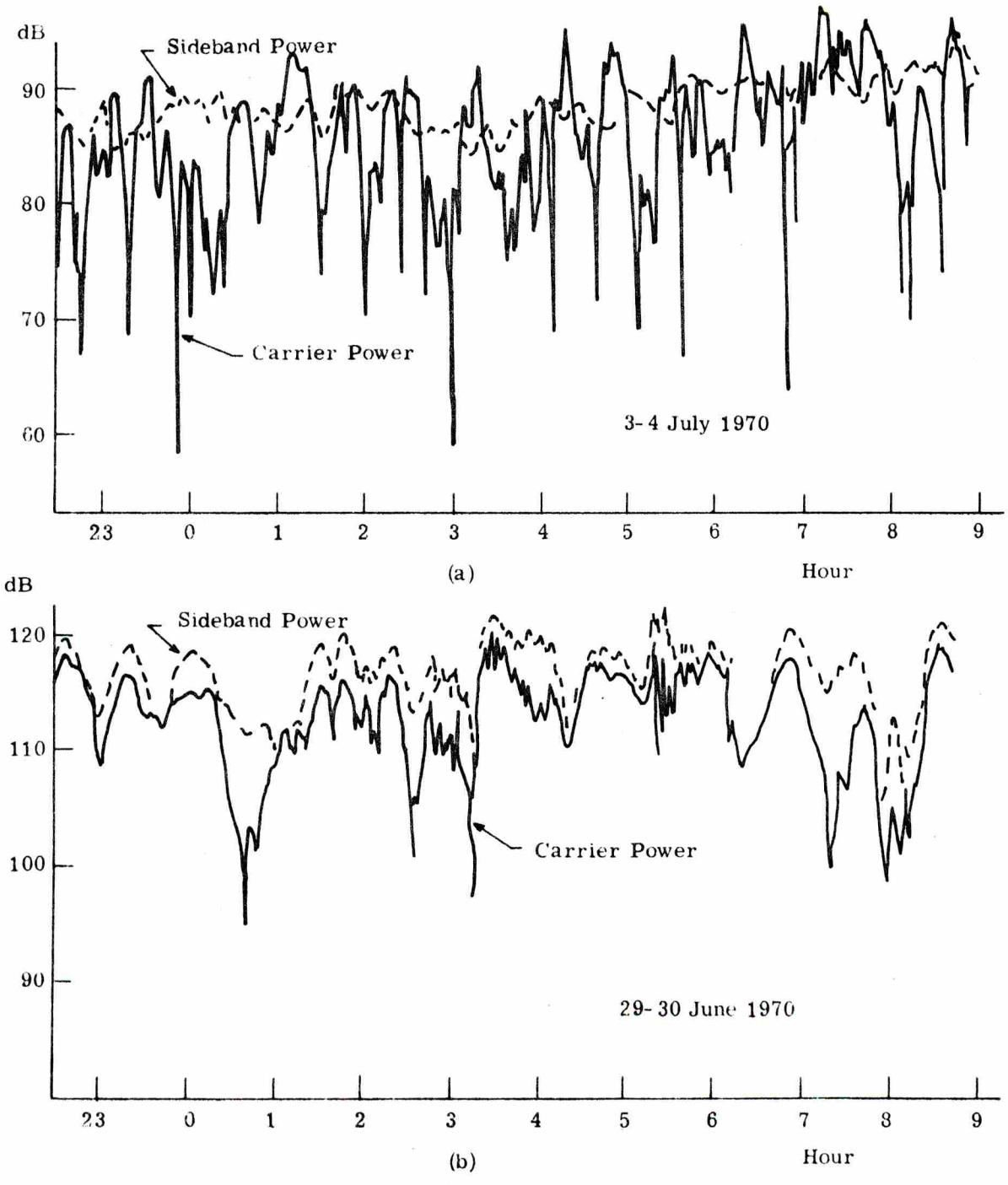

Fig. 13. Unity-gain plots of carrier power and sideband power (a) Bimini hydrophone, (b) 7-mile hydrophone

small portion of the total Bimini data. To illustrate the general character of the power measurements from all of the Bimini data, the slowly varying component of each power has been estimated by computing a sliding average based on a one-half hour averaging time. The plot of these "mean" powers appears on a constant-gain bandwidth scale in Fig. 14.

The most noticeable feature in Fig. 14 is the gradual increase in the levels of both the mean carrier power and the mean sideband power followed by a gradual decrease. Both powers reach the highest levels on the 6th and 7th of July when the signal-to-noise ratios for the carrier power and the sideband power exceed 50 dB and 30 dB respectively. A similar behavior also appears in the mean reverb power although to a lesser extent. The reverb signal-to-noise ratio reaches a maximum of 15 dB for a short period on 6 July. The mean noise power exhibits daily increases and decreases with the maxima occurring during midday and the minima occurring in the late evening and early morning hours.

Examples of the carrier angle measurements from both receiving sites are plotted in cycles (relative to the local reference oscillator) against time in Fig. 15. The carrier angle from the Bimini hydrophone appears in Fig. 15(a). The rate of change of the Bimini carrier angle is typical of the "rapid" changes that occur elsewhere in the Bimini data. This rate of about 12 cycles in 9 hours

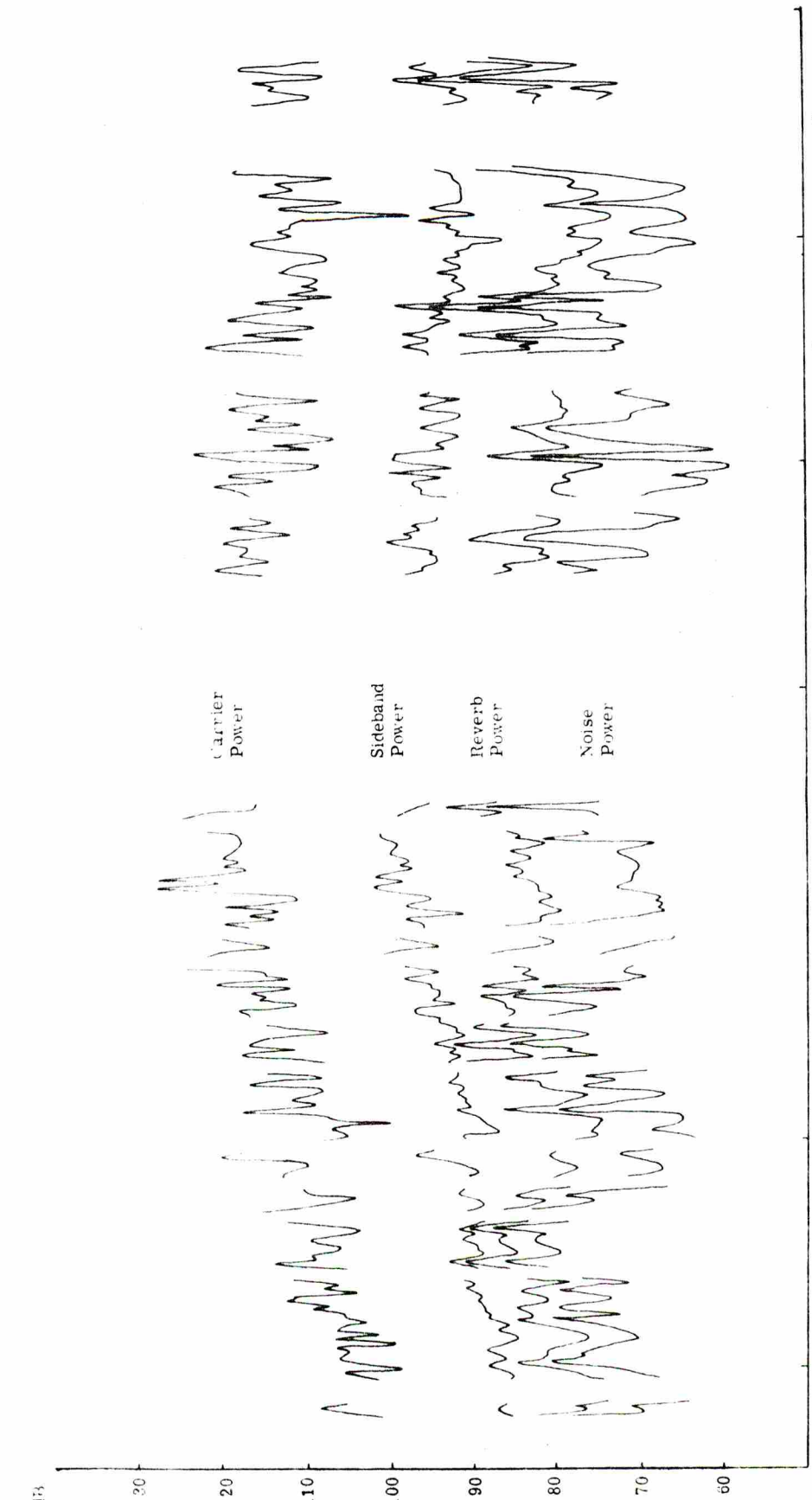

Fig. 14. Mean power plots (1/2 hour averaging time) Date: July 1970

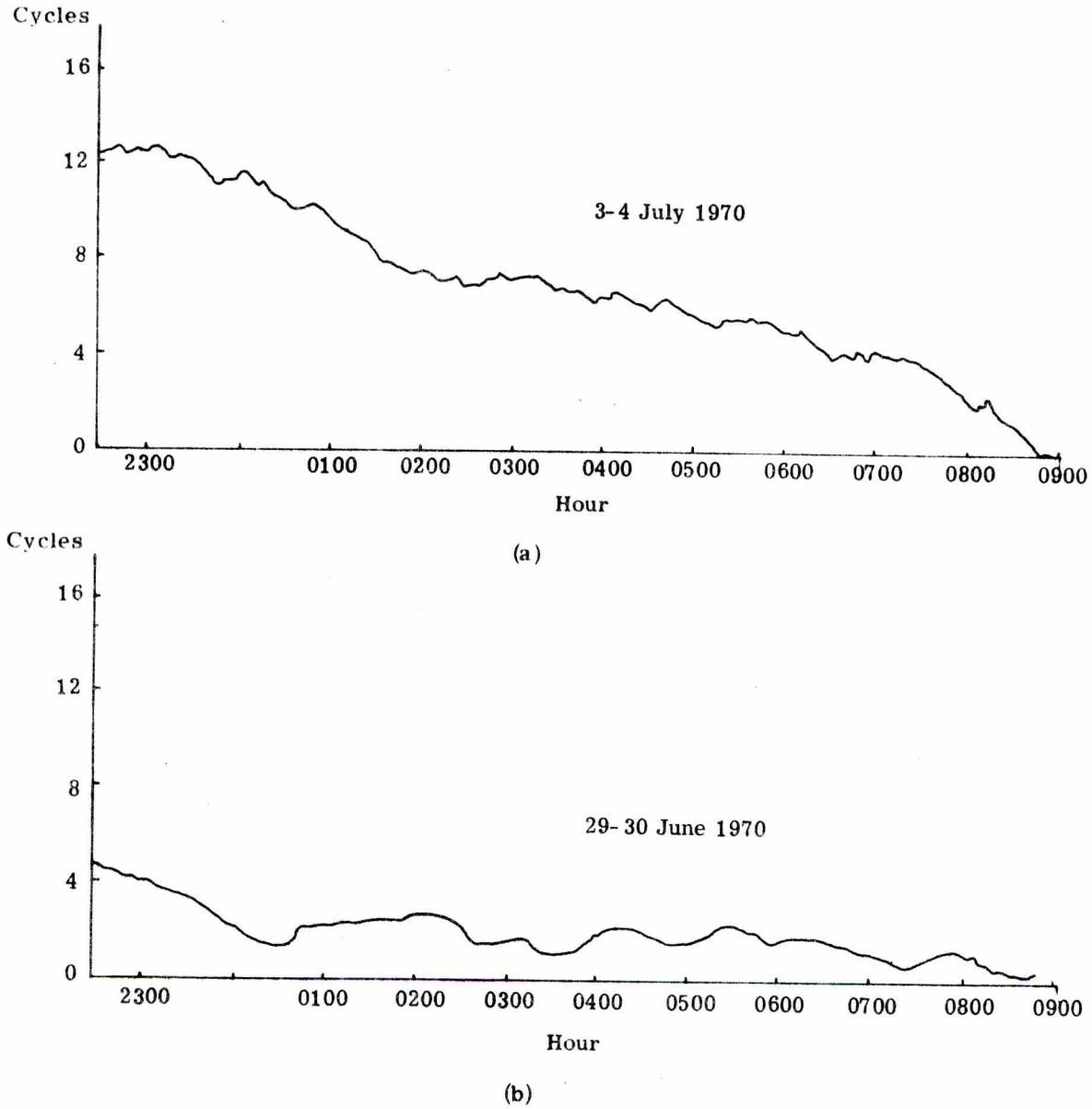

Fig. 15. Carrier angle plot
(a) Bimini hydrophone
(b) 7-mile hydrophone

corresponds to a stability of 1 part in 1.134×10^6 or a frequency shift of 0.00037 Hz.

The carrier angle from the 7-mile hydrophone is illustrated in Fig. 15(b). It is seen that there is only about 1/3 the rate of change in the 7-mile carrier angle although it is not possible to tell if this is typical of 7-mile hydrophone data since no other measurements are available.

2.2 The Surface Reverberation Experiment

The measurements comprising the surface reverberation experiment consist of the reverb power measurement and the reverb spectra. In the preceding section, it was seen that the Bimini reverb signal-to-noise ratio varied between 6 dB and 15 dB, whereas the 7-mile reverb signal-to-noise ratio was approximately 20 dB. Nevertheless, the reverb spectra from both receiving sites did not show a noticeable amount of power in the reverb sidebands as had been expected. It might be mentioned, however, that the seas were unusually calm during the field test, and it is felt that more data are needed before any conclusions can be reached.

2.3 The Multipath Structure Displays

The displays of the multipath structure are obtained as the magnitude of the cross-correlation between the demodulated reception and a pulse-compression reference (Section 1.3). The length

of the time delay axis in these displays is equal to the period of the transmission, 0.59 seconds, and the duration of a single peak in the display is $2d = 0.038$ seconds. (The duration of a single peak is indicated on the top display of each column in each figure.) The vertical scaling for the multipath displays is arbitrary so that care must be used in comparing the relative strengths of arrival peaks in different displays.

Figures 16, 17 and 18 illustrate sequences of multipath displays taken on three successive days from the Bimini data. The time at which each display was taken and the value of the sideband power at that time are indicated next to each display. The multipath displays in Fig. 11 are associated with the lowest values of the sideband power, while those in Fig. 12 are associated with the intermediate values and those in Fig. 13 are associated with the highest values. An examination of these figures indicates a correlation between the number of strong arrival peaks and the value of the sideband power, with the large number of strong arrival peaks being associated with the smaller values of the sideband power. Also note that the spread of the major arrival peaks is greatest when the sideband power is low. Finally, it is seen by examining successive displays in each sequence that the location and amplitudes of the arrival peaks are changing from display to display indicating that the multipath stability is maintained only for periods of the order of minutes.

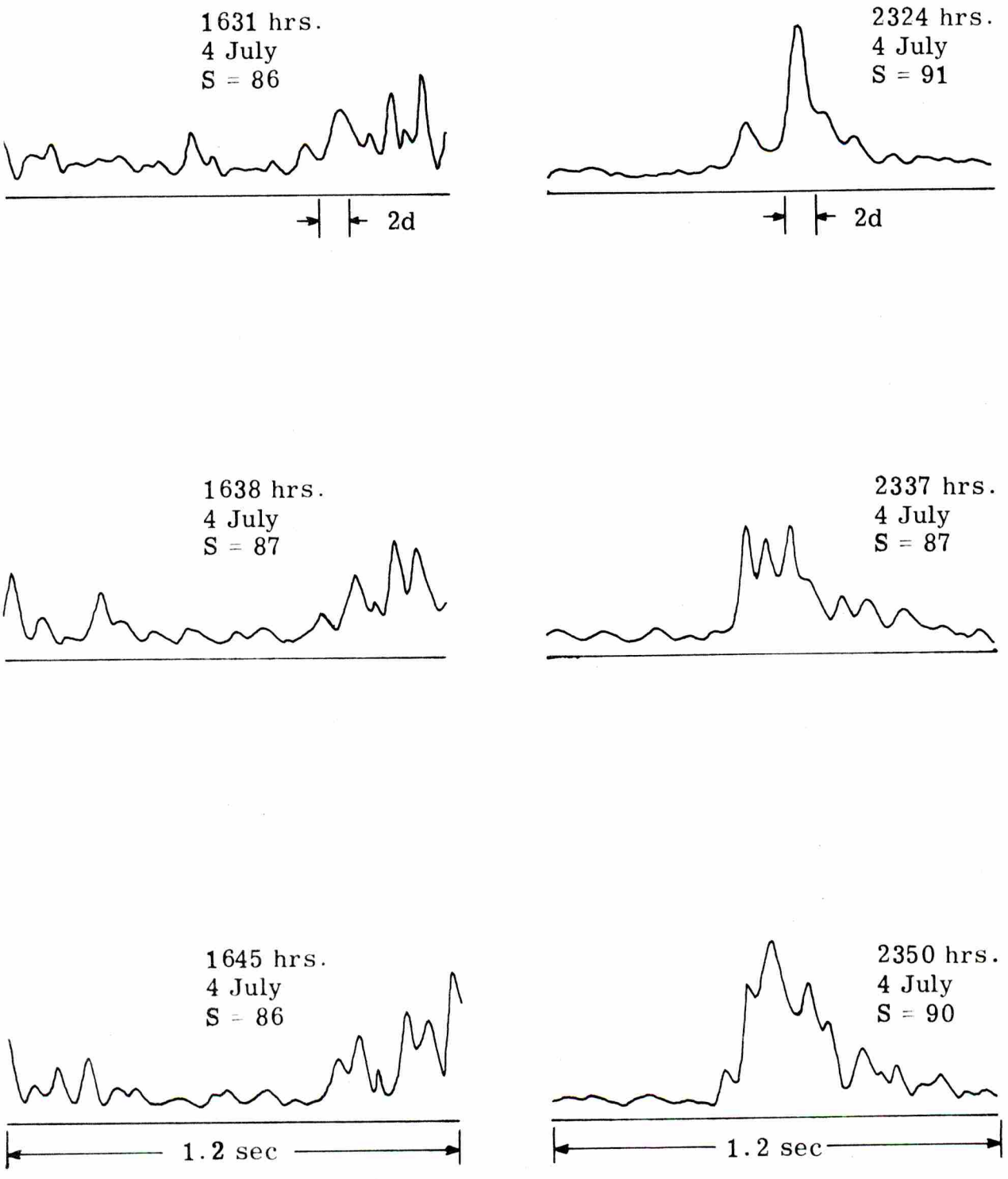

Fig. 16. Multipath displays from the Bimini hydrophone taken on 4 July 1970

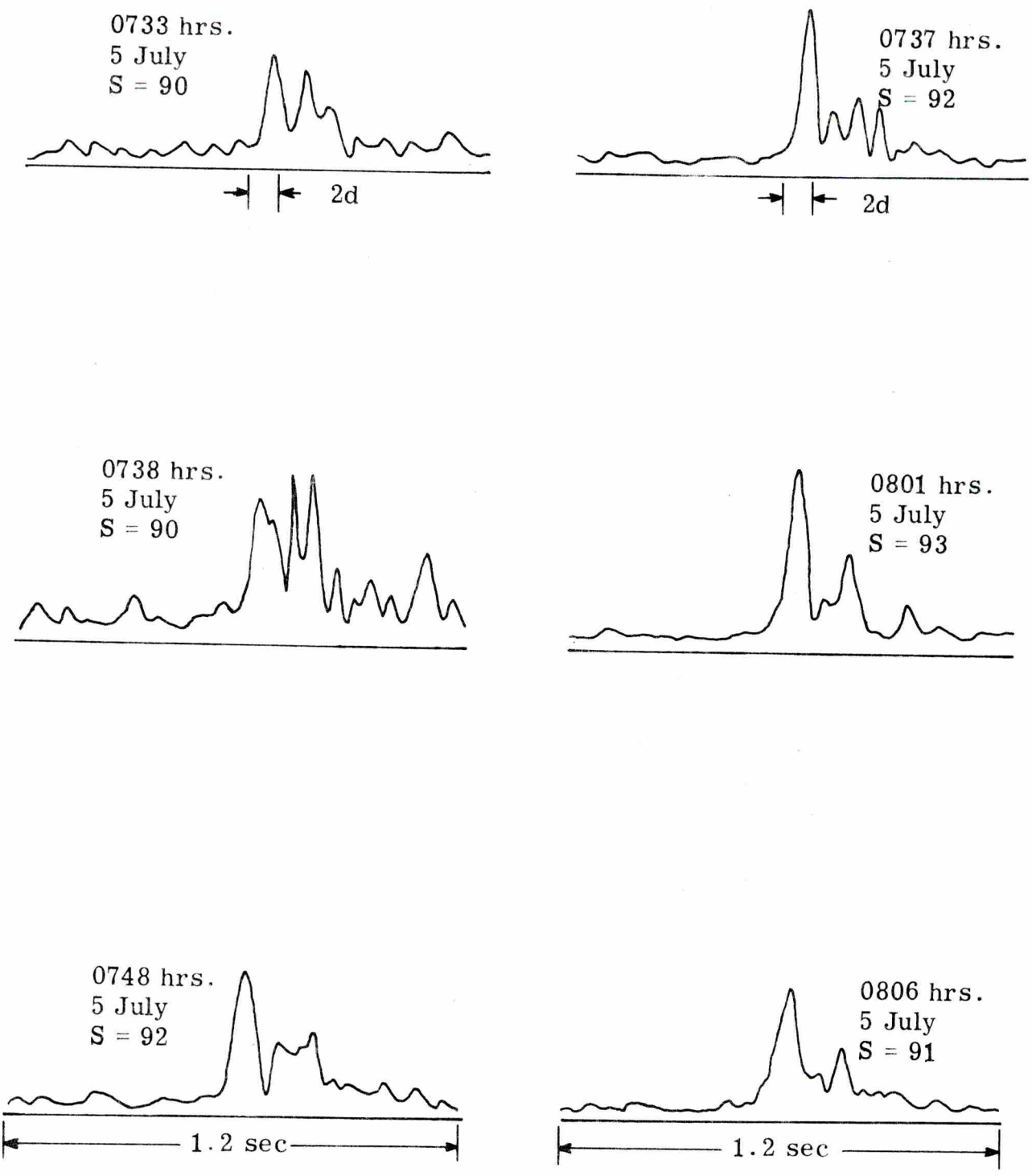

Fig. 17. Multipath displays from the Bimini hydrophone taken on 5 July 1970

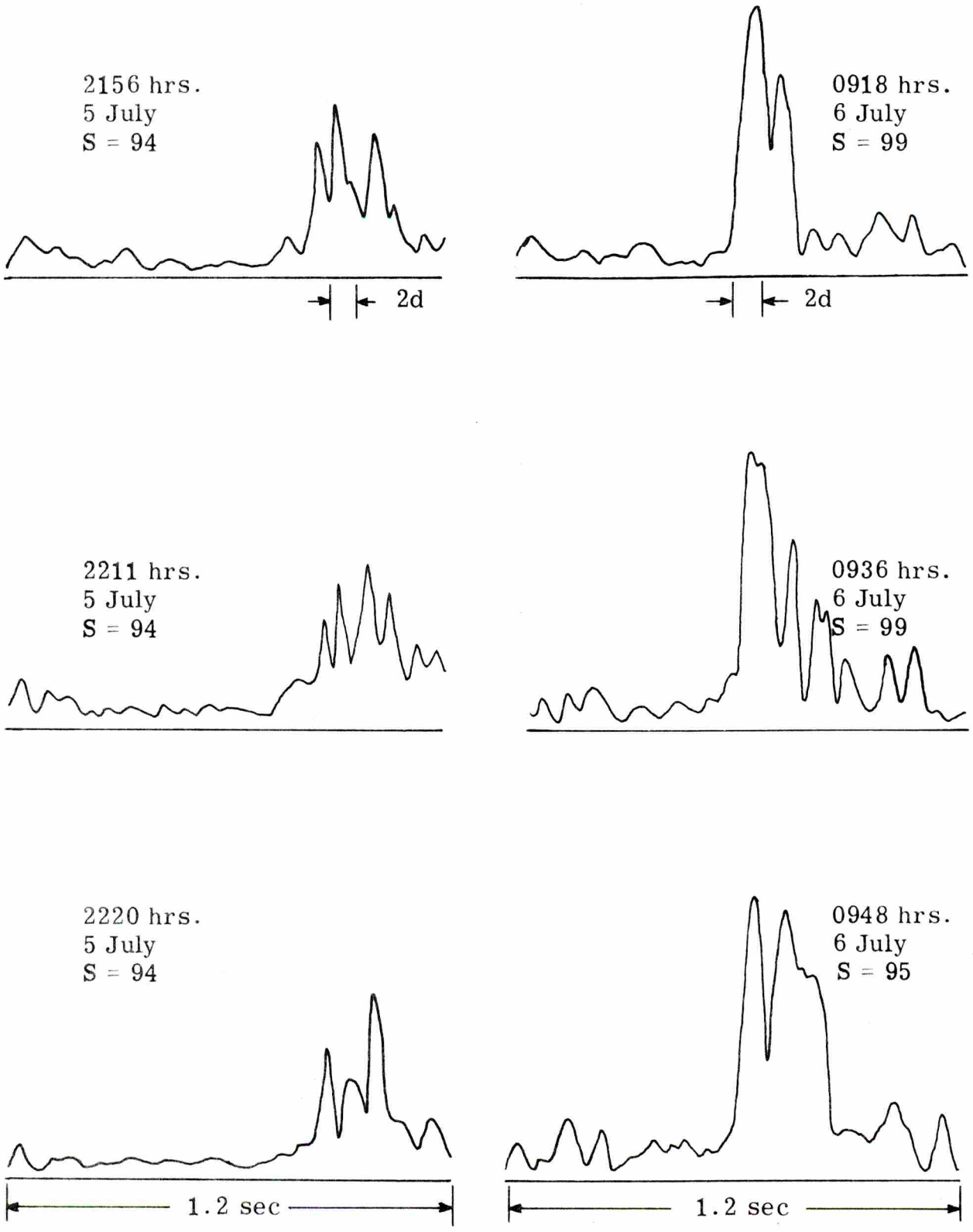

Fig. 18. Multipath displays from the Bimini hydrophone taken on 5-6 July 1970

The technique used to reduce the multipath display data by recomputing new displays only when the correlation coefficient exceeded a threshold, worked as intended with one shortcoming that was not anticipated. Namely, large bursts of shipping noise tended to cause the threshold to be exceeded and a "noisy" multipath display to be stored. In future multipath experiments, it will also be necessary to take into account the current value of the sideband signal-to-noise ratio when thresholding the correlation coefficient.

2.4 Summary and Conclusions

The main purpose of the July 1970 field test was to determine whether or not a portable signal processing unit (the FIELD-8) could be used to run underwater propagation experiments. As a result of the field test, it was seen that this could indeed be done successfully. The FIELD-8 was transported by automobile from Ann Arbor, Michigan to Miami, Florida, set up in the RSMAS Laboratory and run for one day. Then it was transported by charter plane to Bimini, Bahamas, set up and run for eight days and finally returned to Ann Arbor. All of this was done without suffering any equipment failures even though on several occasions the equipment received fairly rough handling. The operation of the equipment proved even easier than had been anticipated since the only task left to the operator was the scheduling of the experiments. Thus, it was concluded that a digital processing unit of this type could be transported and installed with a

high degree of reliability and run with a minimum of operator attention.

The three propagation experiments ran much as had been expected. The processing gains obtained in the FIELD-8 proved sufficient for achieving the necessary signal-to-noise ratios. The amount of variation in the data over the 9-day period, however, suggests that additional experiments be run to determine the long-term behavior of the power and angle measurements. Also, more data are needed to reach a conclusion about the structure of the reverb spectra and the multipath stability. In the future field tests it is felt that the FIELD-8 software package should be rewritten to allow all three experiments to run simultaneously.

DISTRIBUTION LIST

	No. of Copies
Office of Naval Research (Code 468) (Code 102-OS) (Code 480) Navy Department Washington, D. C. 20360	1 1 1
Director, Naval Research Laboratory Technical Information Division Washington, D. C. 20390	6
Director Office of Naval Research Branch Office 1030 East Green Street Pasadena, California 91101	1
Office of Naval Research San Francisco Area Office 1076 Mission Street San Francisco, California 94103	1
Director Office of Naval Research Branch Office 495 Summer Street Boston, Massachusetts 02210	1
Office of Naval Research New York Area Office 207 West 24th Street New York, New York 10011	1
Director Office of Naval Research Branch Office 536 S. Clark Street Chicago, Illinois 60605	1
Director Naval Research Laboratory Attn: Library, Code 2029 (ONRL) Washington, D. C. 20390	8

DISTRIBUTION LIST (Cont.)

	No. of Copies
Commander Naval Ordnance Laboratory Acoustics Division White Oak, Silver Spring, Maryland 20907 Attn: Dr. Zaka Slawsky	1
Commanding Officer Naval Ship Research & Development Center Annapolis, Maryland 21401	1
Commander Naval Undersea Research & Development Center San Diego, California 92132 Attn: Dr. Dan Andrews Mr. Henry Aurand	2
Chief Scientist Navy Underwater Sound Reference Division P. O. Box 8337 Orlando, Florida 32800	1
Commanding Officer and Director Navy Underwater Systems Center Fort Trumbull New London, Connecticut 06321	1
Commander Naval Air Development Center Johnsville, Warminster, Pennsylvania 18974	1
Commanding Officer and Director Naval Ship Research and Development Center Washington, D. C. 20007	1
Superintendent Naval Postgraduate School Monterey, California 93940	1
Commanding Officer & Director Naval Ship Research & Development Center* Panama City, Florida 32402	1

*Formerly Mine Defense Lab.

DISTRIBUTION LIST (Cont.)

	No. of Copies
Naval Underwater Weapons Research & Engineering Station Newport, Rhode Island 02840	1
Superintendent Naval Academy Annapolis, Maryland 21401	1
Scientific and Technical Information Center 4301 Suitland Road Washington, D. C. 20390 Attn: Dr. T. Williams Mr. E. Bissett	2
Commander Naval Ordnance Systems Command Code ORD-03C Navy Department Washington, D. C. 20360	1
Commander Naval Ship Systems Command Code SHIPS 037 Navy Department Washington, D. C. 20360	1
Commander Naval Ship Systems Command Code SHIPS 00V1 Washington, D. C. 20360 Attn: CDR Bruce Gilchrist Mr. Carey D. Smith	2
Commander Naval Undersea Research & Development Center 3202 E. Foothill Boulevard Pasadena, California 91107	1
Commanding Officer Fleet Numerical Weather Facility Monterey, California 93940	1

DISTRIBUTION LIST (Cont.)

	No. of Copies
Defense Documentation Center Cameron Station Alexandria, Virginia 22314	5
Dr. James Probus Office of the Assistant Secretary of the Navy (R&D) Room 4E741, The Pentagon Washington, D. C. 20350	1
Mr. Allan D. Simon Office of the Secretary of Defense DDR&E Room 3E1040, The Pentagon Washington, D. C. 20301	1
CAPT J. Kelly Naval Electronics Systems Command Code EPO-3 Washington, D. C. 20360	1
Chief of Naval Operations Room 5B718, The Pentagon Washington, D. C. 20350 Attn: Mr. Benjamin Rosenberg	1
Chief of Naval Operations Rm 4C559, The Pentagon Washington, D. C. 20350 Attn: CDR J. M. Van Metre	1
Chief of Naval Operations 801 No. Randolph St. Arlington, Virginia 22203	1
Dr. Melvin J. Jacobson Rensselaer Polytechnic Institute Troy, New York 12181	1
Dr. Charles Stutt General Electric Co. P. O. Box 1088 Schenectady, New York 12301	1

DISTRIBUTION LIST (Cont.)

	No. of Copies
Dr. Alan Winder EDO Corporation College Point, New York 11356	1
Dr. T. G. Birdsall Cooley Electronics Lab. University of Michigan Ann Arbor, Michigan 48105	1
Dr. John Steinberg University of Miami Institute of Marine & Atmospheric Sciences Miami, Florida 33149	1
Mr. Robert Cunningham Bendix Corporation 11600 Sherman Way North Hollywood, California 91606	1
Dr. H. S. Hayre University of Houston Cullen Boulevard Houston, Texas 77004	1
Dr. Robert R. Brockhurst Woods Hole Oceanographic Institute Woods Hole, Massachusetts 02543	1
Dr. Stephen Wolff Johns Hopkins University Baltimore, Maryland 21218	1
Dr. M. A. Basin Litton Industries 8000 Woodley Avenue Van Nuys, California 91409	1
Dr. Albert Nuttall Navy Underwater Systems Center Fort Trumbull New London, Connecticut 06320	1

DISTRIBUTION LIST (Cont.)

	No. of Copies
Dr. Philip Stocklin Raytheon Company P. O. Box 360 Newport, Rhode Island 02841	1
Dr. H. W. Marsh Navy Underwater Systems Center Fort Trumbull New London, Connecticut 06320	1
Dr. David Middleton 35 Concord Ave., Apt. #1 Cambridge, Massachusetts 02138	1
Mr. Richard Vesper Perkin-Elmer Corporation Electro-Optical Division Norwalk, Connecticut 06852	1
Dr. Donald W. Tufts University of Rhode Island Kingston, Rhode Island 02881	1
Dr. Loren W. Nolte Dept. of Electrical Engineering Duke University Durham, North Carolina 27706	1
Dr. Thomas W. Ellis Texas Instruments, Inc. 13500 North Central Expressway Dallas, Texas 75231	1
Mr. Robert Swarts Honeywell, Inc. Marine Systems Center 5303 Shilshole Ave., N.W. Seattle, Washington, 98107	1
Mr. Charles Loda Institute for Defense Analyses 400 Army-Navy Drive Arlington, Virginia 22202	1

DISTRIBUTION LIST (Cont.)

	No. of Copies
Mr. Beaumont Buck General Motors Corporation Defense Research Division 6767 Holister Ave. Goleta, California 93017	1
Dr. M. Weinstein Underwater Systems, Inc. 8121 Georgia Avenue Silver Spring, Maryland 20910	1
Dr. Harold Saxton 1601 Research Blvd. TRACOR, Inc. Rockville, Maryland 20850	1
Dr. Thomas G. Kincaid General Electric Company P. O. Box 1088 Schenectady, New York 12305	1
Applied Research Laboratories The University of Texas at Austin Austin, Texas 78712 Attn: Dr. Loyd Hampton Dr. Charles Wood	3
Dr. Paul McElroy Woods Hole Oceanographic Institution Woods Hole, Massachusetts 02543	1
Dr. John Bouyoucos General Dynamics/ Electronics 1400 N. Goodman Street, P. O. Box 226 Rochester, New York 14603	1
Hydrospace Research Corporation 5541 Nicholson Lane Rockville, Maryland 20852 Attn: CDR Craig Olson	1
Cooley Electronics Laboratory University of Michigan Ann Arbor, Michigan 48105	25